

## Research Article

# Topological Transition in a 3 nm Thick Al Film Grown by Molecular Beam Epitaxy

Ankit Kumar,<sup>1,2</sup> Guan-Ming Su,<sup>1</sup> Chau-Shing Chang,<sup>3</sup> Ching-Chen Yeh,<sup>1</sup> Bi-Yi Wu,<sup>1</sup>  
Dinesh K. Patel,<sup>1</sup> Yen-Ting Fan,<sup>4</sup> Sheng-Di Lin<sup>5</sup>,<sup>4</sup> Lee Chow<sup>5</sup>,<sup>1,5</sup> and Chi-Te Liang<sup>1,3</sup>

<sup>1</sup>Department of Physics, National Taiwan University, Taipei 106, Taiwan

<sup>2</sup>Department of Physics, BITS-Pilani, K. K. Birla Goa Campus, Zuarinagar, Goa 403726, India

<sup>3</sup>Graduate Institute of Applied Physics, National Taiwan University, Taipei 106, Taiwan

<sup>4</sup>Department of Electronics Engineering, National Chiao Tung University, Hsinchu 300, Taiwan

<sup>5</sup>Department of Physics, University of Central Florida, Orlando, FL 32816-2385, USA

Correspondence should be addressed to Sheng-Di Lin; [sdlin@mail.nctu.edu.tw](mailto:sdlin@mail.nctu.edu.tw) and Chi-Te Liang; [ctliang@phys.ntu.edu.tw](mailto:ctliang@phys.ntu.edu.tw)

Received 13 June 2019; Accepted 7 September 2019; Published 27 December 2019

Academic Editor: Victor M. Castaño

Copyright © 2019 Ankit Kumar et al. This is an open access article distributed under the Creative Commons Attribution License, which permits unrestricted use, distribution, and reproduction in any medium, provided the original work is properly cited.

We have performed detailed transport measurements on a 3 nm thick (as-grown) Al film on GaAs prepared by molecular beam epitaxy (MBE). Such an epitaxial film grown on a GaAs substrate shows the Berezinskii-Kosterlitz-Thouless (BKT) transition, a topological transition in two dimensions. Our experimental data shows that the MBE-grown Al nanofilm is an ideal system for probing interesting physical phenomena such as the BKT transition and superconductivity. The increased superconductor transition temperature ( $\sim 2.4$  K) compared to that of bulk Al (1.2 K), together with the ultrathin film quality, may be advantageous for future superconductor-based quantum devices and quantum information technology.

## 1. Introduction

The ideas of mathematical topology play an important role in many aspects of quantum physics—from phase transitions to topological insulators [1–4]. In particular, an interesting example of this is the Berezinskii-Kosterlitz-Thouless (BKT) transition—a topological transition from bound vortex-antivortex pairs at low temperatures to unpaired vortices and antivortices at the critical temperature [5, 6]. This elegant model developed by BKT [5, 6] can be used to explain the seemingly forbidden superconducting (ferromagnetic) transition in two dimensions. For a superconducting, topological transition (BKT transition) in two dimensions, at the critical temperature  $T_{\text{BKT}}$ ,  $V \sim I^3$ , where  $V$  and  $I$  are the measured voltage drop between two voltage probes and the driving current flowing between the source and drain contacts, respectively [7]. The BKT transition has been observed in various ultrathin films such as Pb atomic films [8], Ga thin films [9], monolayer NbSe<sub>2</sub> [10], and one-atom-layer Tl-Pb compound on Si (111) [11].

Aluminum (Al) is the most abundant metal on the Earth's crust, and it has already found wide applications in interconnects, coating on graphene, plasmonic devices, and so on [12–14]. Recent advances in sample preparation have made it possible to prepare large-area, high-quality Al films [14, 15]. In particular, large-area Al films with an atomically smooth surface grown by molecular beam epitaxy (MBE) on a GaAs substrate can be readily accessible [15]. Such a high-quality two-dimensional (2D) metallic film is an ideal system for probing 2D physics. Interestingly, the critical temperature  $T_c$  of the studied MBE-grown Al nanofilms ( $\sim 2.4$  K) [15] can be significantly higher than that of bulk Al (1.2 K). In order to obtain a thorough understanding of the physics and the nature of the observed superconductivity in Al nanofilms, we perform detailed transport measurements on a 3 nm thick (as-grown) Al nanofilm. Here, we report experimental evidence for the BKT transition in such a MBE-grown sample. The measured  $T_{\text{BKT}}$  when  $V \sim I^3$  is approximately the critical temperature  $T_c$  determined by the BCS model, unequivocally showing that the observed superconductor transition is a

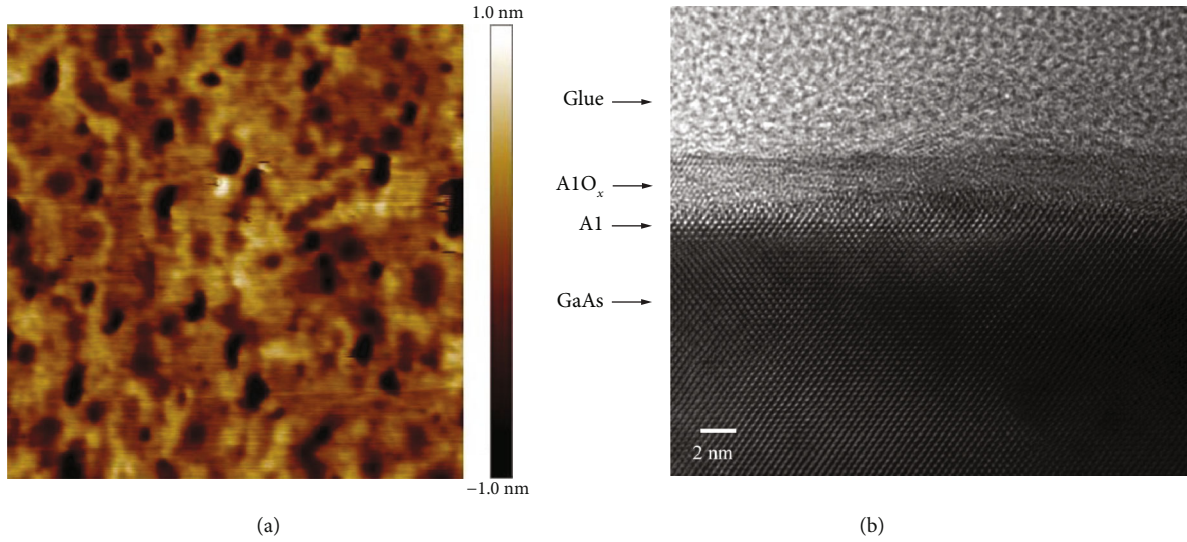


FIGURE 1: (a)  $5\ \mu\text{m} \times 5\ \mu\text{m}$  AFM image of the top surface of the 3 nm thick aluminum film. Note that the scale bar ranges from -1.0 nm to 1.0 nm. (b) Cross-sectional TEM image of the as-grown 3 nm thick Al film grown by MBE.

topological transition in two dimensions. Although superconductivity in Al thin films has been studied in depth [16], our Al nanofilms are grown on GaAs; therefore, it is possible for one to combine superconducting devices with GaAs-based transistors and high-frequency devices on the *same* substrate. Such an advantage may be useful for future quantum information processing and computation technology.

## 2. Experimental Section

The 3 nm thick Al film reported in this paper was prepared in a Varian Gen-II solid-source MBE system [15]. The experimental details can be found in the supplementary information (S1). The quality of the sample in this work is similar to those reported in Ref. [15]. In our earlier work, for a MBE-grown film deposited at room temperature with an intended thickness of 3 nm, the average roughness of the film is about 4.9 nm which is thicker than the deposited thickness and is possibly caused by the Al oxidation after the exposure to air [17]. In contrast, the surface roughness of the current Al nanofilm grown below  $0^\circ\text{C}$  is more than an order of magnitude lower (see Figure 1(a)). Therefore, we believe that the substrate temperature is the key issue for preparing a high-quality MBE-grown Al nanofilm: the lower the substrate temperature, the higher the sample quality (the lower the surface roughness).

We chose to study a 3 nm thick Al film as this is the thinnest conducting sample which we can prepare. If the as-grown thickness is below 3 nm, for example, say 2.5 nm, the film becomes nonconducting even at room temperature, suggesting that the thin film may be discontinuous. For the current experiments, the sample was processed into a Hall bar geometry (see Supplementary Information S2).

## 3. Results and Discussion

Figure 1(a) shows a  $5\ \mu\text{m} \times 5\ \mu\text{m}$  atomic force microscope (AFM) top-view image of the 3 nm thick Al film in air. The

root mean square (RMS) roughness is about 0.29 nm. This low RMS surface roughness demonstrates that our film is of high quality. The black regions may correspond to voids in the Al nanofilm which are not conducting and should not affect the transport properties and superconductivity in our Al nanofilm.

Figure 1(b) shows a cross-sectional transmission electron microscope (TEM) image. A nearly defect-free Al film of thickness of  $\sim 1$  nm can be observed. According to the TEM data shown in Figure 1(b), although the as-grown thickness of our Al film is 3 nm, the actual conducting layer is about 1 nm thick due to the formation of the  $\sim 2$  nm thick  $\text{AlO}_x$  layer on top of the aluminum film. Such an  $\text{AlO}_x$  layer can prevent the Al nanofilm from further oxidation. An  $\text{AlO}_x$  overlaying layer may introduce strain to the Al nanofilm, though this layer is present in most Al films in the literature.

The MBE-grown Al nanofilm was processed into Hall bars, and standard dc four-terminal resistance measurements were performed on our Al samples (please see Supplementary Information S3). Figure 2(a) shows the square resistance measurements as a function of magnetic field  $R_s(H)$  of a 3 nm thick Al device at various temperatures  $T$ . The magnetic field  $H$  is applied perpendicular to the plane of the Al film. At the lowest temperature of 0.25 K,  $R_s$  is zero when  $|H| \leq 1.23$  T. For  $|H| > 1.23$  T,  $R_s$  starts to increase and reaches saturation (the normal state where  $R_N$  is about 1650  $\Omega$ ) at around 3 T. When  $R_s(H)$  is half of the normal state value  $R_N/2$ , we can determine the critical magnetic field  $H_c(T = 0.25\ \text{K})$  to be 1.47 T. By repeating this procedure for various temperatures,  $H_c(T)$  can be measured, and such results are shown in Figure 2(b). There is a good fit  $H_c = H_{c0}[1 - (T/T_{\text{BCS}})^2]$  based on the Gorter-Casimir theory [18] which is strongly related to the BCS model [19] to the data. According to the fit to our experimental data, we can determine the critical magnetic field  $H_{c0}$  and critical temperature  $T_{\text{BCS}}$  to be 1.51 T and 2.40 K, respectively. We note that in the normal state in the high magnetic field regime,  $R_N$  tends to decrease

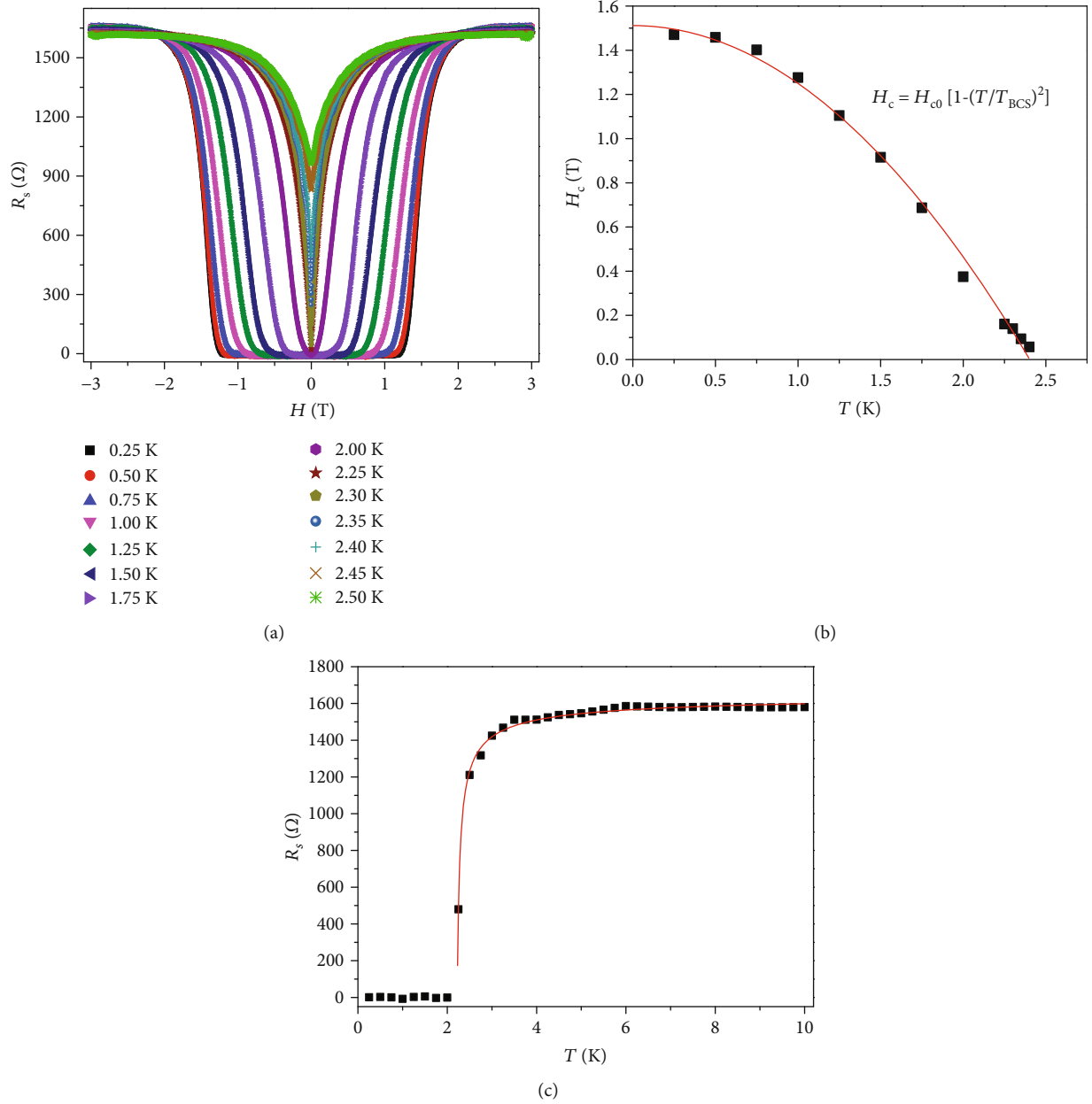


FIGURE 2: (a) Square resistance measurements as a function of magnetic field  $R_s(H)$  at different temperatures. (b) Critical magnetic field  $H_c$  as a function of temperature  $T$ . The red curve corresponds to a fit based on the BCS model to the experimental data. (c)  $R_s$  as a function of temperature at  $H=0$ . The red curve corresponds to the fit to Equations (1) and (2) based on the Aslamazov-Larkin-Maki-Thompson correction.

slightly with increasing temperature  $T$ , showing weak semiconductor-like behavior [20–22]. Similar results have been observed in monolayer NbSe<sub>2</sub> [10], ultrathin crystalline lead films [23], and a two-atom layer of hexagonal Ga film grown on semiconducting GaN(0001) [24]. A possible reason for these results is that the sample shows a weak localization effect when increasing the measurement temperature.

In order to further study the observed superconducting transition,  $R_s(T)$  over a wider range of temperature is shown in Figure 2(c). We are now able to fit out data to the following equations based on the Aslamazov-Larkin- (AL-) Maki-Thompson (MT) correction as described in Ref. [25]:

$$\rho = \frac{1}{\sigma_0 + \sigma_{AL} + \sigma_{MT}^{ano}}. \quad (1)$$

Here,  $\sigma_{AL}$  and  $\sigma_{MT}^{ano}$  are given by

$$\sigma_{AL} = \frac{\pi e^2}{8h} \frac{T_c}{T - T_c}, \quad (2)$$

$$\sigma_{MT}^{ano} = \frac{\pi e^2}{4h} \frac{T_c}{T - (1 + \delta)T_c} \ln \frac{T - T_c}{\delta T_c}, \quad (3)$$

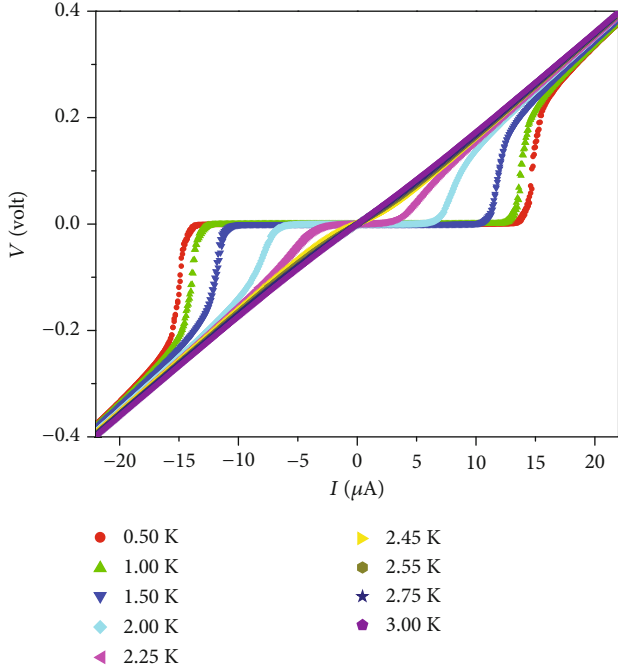


FIGURE 3: The  $I$ - $V$  characteristics of a 3 nm thick Al film at different temperatures.

where  $\delta$  is the phase-breaking parameter. According to the red curve which corresponds to the fit to Equations (1), (2) and (3),  $T_c$  and  $\delta$  of our 3 nm thick Al film are measured to be 2.21 K and 0.775. The estimated  $\delta$  is close to that predicted (0.993) in Ref. [26].

Figure 3 shows the four-terminal  $I$ - $V$  characteristics of the 3 nm thick Al nanofilm at different temperatures. At  $T = 0.5$  K, a dissipationless current, i.e., a supercurrent, can be observed. There is a superconductor-metal transition at around  $I = 13.7 \mu\text{A}$ , where we observe an abrupt increase in the measured voltage. With increasing temperature, the supercurrent is decreased. At  $T = 2.25$  K, there exists a low supercurrent, showing that the device is still superconducting. Such an elevated transition temperature is highly useful for our superconducting devices grown on GaAs as we can integrate superconductor-based devices with GaAs-based high-electron mobility transistors (HEMTs) and high-frequency transistors on the same GaAs substrate.

In order to further probe the superconductor transition, we perform detailed  $V(I)$  measurements at various temperatures. Figure 4 shows such results on a log-log scale. The red lines correspond to fits  $V \sim I^\alpha$  to experimental data at various temperatures. The black line corresponds to  $V \sim I^3$  when the BKT transition occurs. The measured exponent  $\alpha$  as a function of temperature is shown in Figure 5. By interpolation, we can determine the topological transition temperature  $T_{\text{BKT}}$  to be 2.29 K at  $V \sim I^3$ , which is in close agreement with the measured  $T_{\text{BCS}} = 2.4$  K and the critical temperature based on the Aslamazov-Larkin-Maki-Thompson correction  $T_c = 2.21$  K in the linear regime. Our experimental results clearly show that the observed superconductor transition in our Al nanofilm is a topological transition in two dimensions,

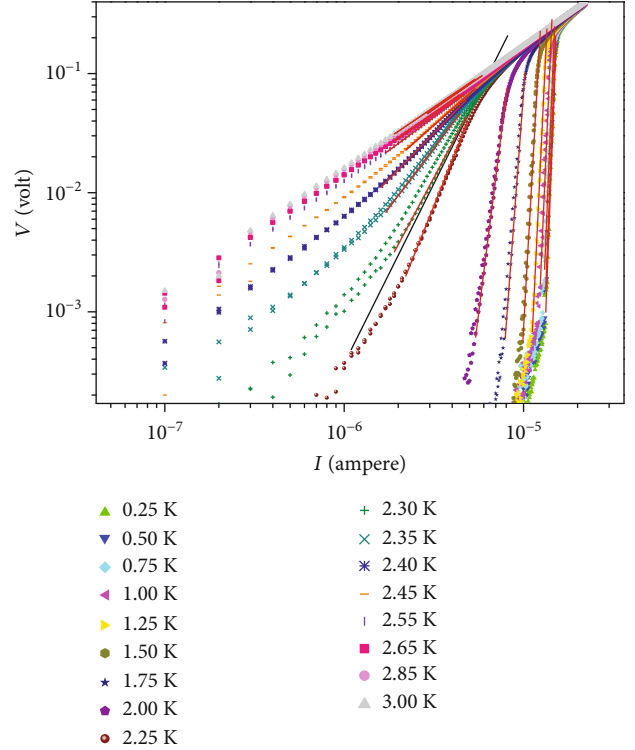


FIGURE 4:  $I$ - $V$  curves at various temperatures on a log-log scale. The red lines correspond to linear fits  $V \sim I^\alpha$  to the experimental data. The black line corresponds to  $V \sim I^3$ .

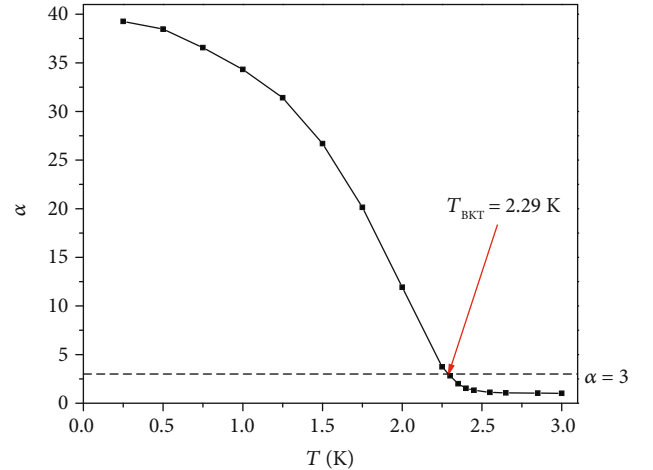


FIGURE 5: The measured exponent  $\alpha$  determined from the relation  $V \sim I^\alpha$  at various temperatures  $T$ . The experimentally determined BKT transition temperature is estimated to be  $T = 2.29$  K when  $V \sim I^3$ .

and our data can be described by both the Gorter-Casimir theory related to the BCS model and the Aslamazov-Larkin-Maki-Thompson correction.

Normally, the superconducting transition temperature of a thin film is lower than that of a bulk sample. We note that



the opposite trend (increased  $T_c$  measured in thin films compared to those of bulk samples) has been observed in double-atomic-layer Ga films on GaN [24], FeSe monolayer films on SrTiO<sub>3</sub> [27], and FeSe on TiO<sub>2</sub> [28]. These interesting results, together with the present work on the MBE-grown Al nanofilm, may suggest that the interface effects play a significant role in the enhanced superconductor transition temperature in a thin film over that of its bulk counterpart [29].

#### 4. Conclusion

In conclusion, we have performed extensive transport measurements on a 3 nm thick (as-grown) Al film grown on a GaAs substrate by MBE. Such a MBE-grown Al nanofilm is of high quality as demonstrated by both AFM and TEM measurements. Importantly, we have observed the BKT transition in two dimensions as evidenced by  $V \sim I^3$  in the nonlinear  $I$ - $V$  regime. The measured topological transition temperature  $T_{\text{BKT}} \sim 2.29$  K is close to the critical temperature  $T_{\text{BCS}} \sim 2.4$  K as determined by the Gorter-Casimir theory strongly related to the BCS model as well as the transition temperature based on the Aslamazov-Larkin-Maki-Thompson correction  $T_c \sim 2.21$  K. The higher transition temperature compared to that of bulk Al (1.2 K) is highly desirable for possible future superconductor-based quantum computation scheme and quantum devices. Moreover, our high-quality Al film is fully compatible with the existing GaAs-based HEMT technology; thus, our experimental results may open the way for combination of superconducting devices and HEMT devices.

#### Data Availability

The data used to support the findings of this study are available from the corresponding authors upon request.

#### Conflicts of Interest

The authors declare that they have no conflicts of interest.

#### Authors' Contributions

Ankit Kumar and Guan-Ming Su contributed equally to this work.

#### Acknowledgments

The authors acknowledge the technical support from the Center of Nano Science and Technology and the Center of Nano Facility at National Chiao Tung University, Integrated Service Technology Co. Ltd., and National Device Laboratory. This work was financially supported by the Ministry of Education (MOE) ATU program, National Taiwan University (NTU) (grant numbers 107L892101 and 108L892101), and the Ministry of Science and Technology (MOST) (grant numbers MOST 105-2112-M-002-005-MY3, MOST 108-2112-M-002-014-MY2, and MOST 108-2622-8-002-016), Taiwan. L.C. acknowledges the hospitality of the Physics Department of NTU during his sabbatical stay at NTU. The work of A.K. at NTU was made possible by

arrangement with Prof. E. S. Kannan at BITS-Pilani, India. A.K. was supported by the TEEP@India Program provided by the MOE, Taiwan (grant number 106M4102-7).

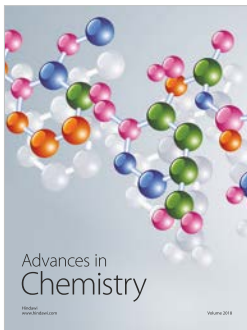
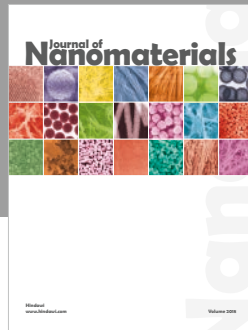
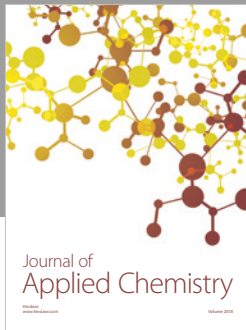
#### Supplementary Materials

S1: MBE growth of Al nanofilm. S2: device geometry and stability. S3: low-temperature resistance measurements. (*Supplementary Materials*)

#### References

- [1] C. L. Kane and E. J. Mele, "Z<sub>2</sub> topological order and the quantum spin Hall effect," *Physical Review Letters*, vol. 95, no. 14, article 146802, 2005.
- [2] B. A. Bernevig, T. L. Hughes, and S. C. Zhang, "Quantum spin Hall effect and topological phase transition in HgTe quantum wells," *Science*, vol. 314, no. 5806, pp. 1757–1761, 2006.
- [3] M. König, S. Wiedmann, C. Brüne et al., "Quantum spin Hall insulator state in HgTe quantum wells," *Science*, vol. 318, no. 5851, pp. 766–770, 2007.
- [4] H. N. S. Krishnamoorthy, Z. Jacob, E. Narimanov, I. Kretzschmar, and V. M. Menon, "Topological transitions in metamaterials," *Science*, vol. 336, no. 6078, pp. 205–209, 2012.
- [5] V. L. Berezinskii, "Destruction of long range order in one-dimensional and two-dimensional systems having a continuous symmetry group. I. Classical systems," *Zhurnal Eksperimental'noi i Teoreticheskoi Fiziki*, vol. 59, p. 907, 1970.
- [6] J. M. Kosterlitz and D. J. Thouless, "Ordering, metastability and phase transitions in two-dimensional systems," *Journal of Physics C*, vol. 6, no. 7, article 1181, 1203 pages, 1973.
- [7] K. Epstein, A. M. Goldman, and A. M. Kadin, "Vortex-antivortex pair dissociation in two-dimensional superconductors," *Physical Review Letters*, vol. 47, no. 7, pp. 534–537, 1981.
- [8] W. Zhao, Q. Wang, M. Liu et al., "Evidence for Berezinskii-Kosterlitz-Thouless transition in atomically flat two-dimensional Pb superconducting films," *Solid State Communications*, vol. 165, pp. 59–63, 2013.
- [9] Y. Xing, H.-M. Zhang, H.-L. Fu et al., "Quantum Griffiths singularity of superconductor-metal transition in Ga thin films," *Science*, vol. 350, no. 6260, pp. 542–545, 2015.
- [10] H. Wang, X. Huang, J. Lin et al., "High-quality monolayer superconductor NbSe<sub>2</sub> grown by chemical vapour deposition," *Nature Communications*, vol. 8, no. 1, p. 394, 2017.
- [11] A. V. Matetskiy, S. Ichinokura, L. V. Bondarenko et al., "Two-dimensional superconductor with a giant Rashba effect: one-atom-layer TI-Pb compound on Si (111)," *Physical Review Letters*, vol. 115, no. 14, article 147003, 2015.
- [12] Z. Y. Zhao, R. D. K. Misra, P. K. Bai et al., "Novel process of coating Al on graphene involving organic aluminum accompanying microstructure evolution," *Materials Letters*, vol. 232, pp. 202–205, 2018.
- [13] B.-T. Chou, Y.-H. Chou, Y.-M. Wu et al., "Single-crystalline aluminum film for ultraviolet plasmonic nanolasers," *Scientific Reports*, vol. 6, no. 1, article 19887, 2016.
- [14] C.-W. Cheng, Y.-J. Liao, C.-Y. Liu et al., "Epitaxial aluminum-on-sapphire films as a plasmonic material platform for ultraviolet and full visible spectral regions," *ACS Photonics*, vol. 5, no. 7, pp. 2624–2630, 2018.

- [15] Y.-T. Fan, M.-C. Lo, C.-C. Wu et al., “Atomic-scale epitaxial aluminum film on GaAs substrate,” *AIP Advances*, vol. 7, no. 7, article 075213, 2017.
- [16] R. Meservey and P. M. Tedrow, “Properties of very thin aluminum films,” *Journal of Applied Physics*, vol. 42, no. 1, pp. 51–53, 1971.
- [17] S.-W. Lin, Y.-H. Wu, L. Chang, C.-T. Liang, and S.-D. Lin, “Pure electron-electron dephasing in percolative aluminum ultrathin film grown by molecular beam epitaxy,” *Nanoscale Research Letters*, vol. 10, no. 1, article 71, 2015.
- [18] J. C. Gorter and H. B. Casimir, “The thermodynamics of the superconducting state,” *Physikalische Zeitschrift*, vol. 35, p. 963, 1934.
- [19] J. Bardeen, L. N. Cooper, and J. R. Schrieffer, “Theory of superconductivity,” *Physics Review*, vol. 108, no. 5, pp. 1175–1204, 1957.
- [20] J.-H. Chen, J.-Y. Lin, J.-K. Tsai et al., “Experimental evidence for Drude-Boltzmann-like transport in a two-dimensional electron gas in an AlGa<sub>N</sub>/Ga<sub>N</sub> heterostructure,” *Journal of Korean Physic Society*, vol. 48, no. 6, pp. 1539–1543, 2006.
- [21] J. R. Juang, T.-Y. Huang, T.-M. Chen et al., “Transport in a gated Al<sub>0.18</sub>Ga<sub>0.82</sub>N/GaN electron system,” *Journal of Applied Physics*, vol. 94, no. 5, pp. 3181–3184, 2003.
- [22] C. Chuang, M. Mineharu, N. Matsumoto et al., “Hot carriers in CVD-grown graphene device with a top h-BN layer,” *Journal of Nanomaterials*, vol. 2018, Article ID 5174103, 7 pages, 2018.
- [23] Y. Liu, Z. Wang, X. Zhang et al., “Interface-induced Zeeman-protected superconductivity in ultrathin crystalline lead films,” *Physical Review X*, vol. 8, article 021002, 2018.
- [24] H.-M. Zhang, Y. Sun, W. Li et al., “Detection of a superconducting phase in a two-atom layer of hexagonal Ga film grown on semiconducting GaN(0001),” *Physical Review Letters*, vol. 114, no. 10, article 107003, 2015.
- [25] M. Yamada, T. Hirahara, and S. Hasegawa, “Magnetoresistance measurements of a superconducting surface state of In-induced and Pb-induced structures on Si (111),” *Physical Review Letters*, vol. 110, no. 23, article 237001, 2013.
- [26] K. Kajimura and N. Mikoshiba, “Fluctuations in the resistive transition in aluminum films,” *Journal of Low Temperature Physics*, vol. 4, no. 3, pp. 331–348, 1971.
- [27] J.-F. Ge, Z.-L. Liu, C. Liu et al., “Superconductivity above 100 K in single-layer FeSe films on doped SrTiO<sub>3</sub>,” *Nature Materials*, vol. 14, no. 3, pp. 285–289, 2015.
- [28] H. Ding, Y.-F. Lv, K. Zhao et al., “High-temperature superconductivity in single-unit-cell FeSe films on AnataseTiO<sub>2</sub>(001),” *Physical Review Letters*, vol. 117, no. 6, article 067001, 2016.
- [29] A. Eich, N. Rollfing, F. Arnold et al., “Absence of superconductivity in ultrathin layers of FeSe synthesized on a topological insulator,” *Physical Review B*, vol. 94, no. 12, article 125437, 2016.



**Hindawi**  
Submit your manuscripts at  
[www.hindawi.com](http://www.hindawi.com)

